

## Cationic Pentaheteroaryls as Selective G-Quadruplex Ligands by Solvent-Free Microwave-Assisted Synthesis

Michele Petenzi,<sup>[a]</sup> Daniela Verga,<sup>[b]</sup> Eric Largy,<sup>[b]</sup> Florian Hamon,<sup>[b]</sup> Filippo Doria,<sup>[a]</sup> Marie-Paule Teulade-Fichou,<sup>\*[b]</sup> Aurore Guédin,<sup>[c]</sup> Jean-Louis Mergny,<sup>[c]</sup> Mariella Mella,<sup>[a]</sup> and Mauro Freccero<sup>\*[a]</sup>

**Abstract:** We report herein a solvent-free and microwaved-assisted synthesis of several water soluble acyclic pentaheteroaryls containing 1,2,4-oxadiazole moieties (1–7). Their binding interactions with DNA quadruplex structures were thoroughly investigated by FRET melting, fluorescent intercalator displacement assay (G4-FID) and CD spectroscopy. Among the G-quadruplexes considered, attention was fo-

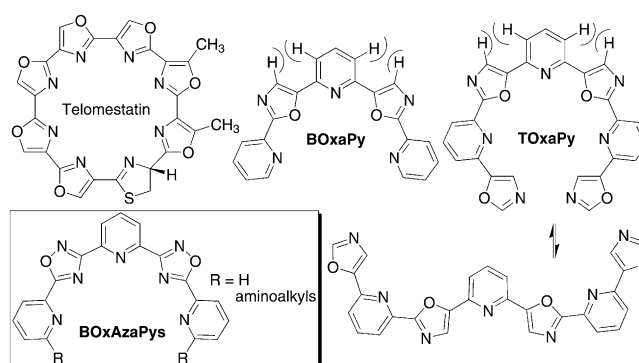
ocused on telomeric repeats together with the proto-oncogenic *c-kit* sequences and the *c-myc* oncogene promoter.

**Keywords:** 1,2,4-oxadiazoles • DNA recognition • G-quadruplexes • microwave chemistry • pentaheteroaryls

Compound 1, and to a lesser extent 2 and 5, preferentially stabilise an anti-parallel structure of the telomeric DNA motif, and exhibit an opposite binding behaviour to structurally related polyoxazole (TOxaPy), and do not bind duplex DNA. The efficiency and selectivity of the binding process was remarkably controlled by the structure of the solubilising moieties.

### Introduction

Organic compounds capable of recognising and stabilising the G-quadruplex supramolecular structure of nucleic acids (G4) have attracted great attention as selective probes and anticancer agents.<sup>[1]</sup> Beside a large array of reversible ligands,<sup>[1b,2]</sup> selective G4 alkylating agents are beginning to emerge.<sup>[3]</sup> Dual selectivity towards quadruplex versus duplex DNA and different quadruplex architectures is a key aspect for developing effective diagnostic and pharmacological applications for G4 ligands.<sup>[4]</sup> The selectivity issue is still propelling the design of new G4 binders. In spite of the large variety of synthetic ligands created to date, the natural macrocycle telomestatin (Scheme 1) still exhibits a unique neutral molecular architecture, combining excellent binding, selectivity and remarkable antitumor activity.<sup>[5]</sup> Its structural features are still inspiring the design and synthesis of a large number of both cyclic and acyclic polyheterocyclic ligands.<sup>[6]</sup>



Scheme 1. Cyclic and acyclic polyheteroaryl ligands based on oxazoles and the prototype **BOxAzaPy** (R=H) together with the water soluble analogues (R=H, aminoalkyls) embedding 1,2,4-oxadiazole moieties (**BOxAzaPy**).

Several of them, including the recent **TOxaPy**, exhibit polyoxazole structures.<sup>[7]</sup> The potentials of acyclic derivatives as G4 ligands have been highlighted by an unexpected specificity of **TOxaPy** (Scheme 1), resulting probably from groove interactions.<sup>[7]</sup> The binding properties were strongly dependent on the length of the oligomeric ligand, as the shorter pentaheteroaryl **BOxaPy** did not bind to G4 targets. In order to systematically investigate the full potential of acyclic polyheterocyclic structures as G4 ligands, we began a joint project in which some of us designed and synthesised a family of a fairly similar scaffold containing 1,2,4-oxadiazole moieties.

Water solubility of the resulting pentaheteroaryls was achieved by two symmetric and structurally modular aminoalkyl or hydroxy-alkyl groups (**BOxAzaPy** compounds, Scheme 1), introduced by an efficient microwave-assisted

[a] M. Petenzi, Dr. F. Doria, Prof. M. Mella, Prof. M. Freccero  
Dipartimento di Chimica, Università di Pavia  
V.le Taramelli 10, 27100 Pavia (Italy)  
Fax: (+39)0382987668  
E-mail: mauro.freccero@unipv.it

[b] Dr. D. Verga, Dr. E. Largy, Dr. F. Hamon, Dr. M.-P. Teulade-Fichou  
UMR176 CNRS, Institut Curie, Centre de Recherche  
Centre Universitaire, 91405 Orsay (France)  
Fax: (+33)169-07-53-81  
E-mail: marie-paule.teulade-fichou@curie.fr

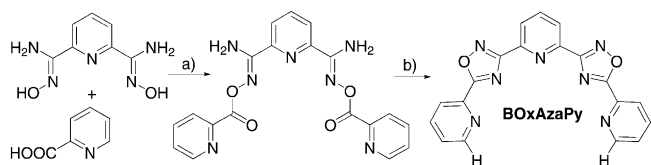
[c] A. Guédin, Dr. J.-L. Mergny  
Université de Bordeaux, INSERM U869  
IECB, 2 rue Robert Escarpit, 33600 Pessac (France)

Supporting information for this article is available on the WWW under <http://dx.doi.org/10.1002/chem.201202097>.

functionalisation of the prototype **BOxAzaPy** scaffold. The replacement of the oxazoles by 1,2,4-oxadiazoles should, in principle: 1) allow the formation of a nitrogen binding cavity in the bent conformer, such as in the telomestatin-like ligands, and 2) erase the CH–CH steric repulsions within the oxazole-based oligoheteroaryls, like **BOxApy** and **TOxApy**. The above structural features, including the cationic appendages, could have a strong impact on the binding mode of the new polyheterocycles toward G4. This aspect has been thoroughly investigated in the present study. Finally, in order to fully compare the oxazole and oxadiazole series, we prepared three cationic derivatives of **BOxApy** (**8–10**) bearing side chains similar to those embedded in the **BOxAzaPy** series.

## Results and Discussion

**One step synthesis of the prototype BOxAzaPy:** Several methods are currently available for the synthesis of mono-functional 1,2,4-oxadiazoles. Among these, the condensation of amidoxime with carboxylic acids in the presence of a coupling reagent is often considered particularly attractive.<sup>[8]</sup> We chose 1,1'-carbonyldiimidazole (CDI) as a coupling reagent because the subsequent cyclodehydration can be easily performed one-pot in the presence of the same CDI, in DMF, without isolation of the resulting *O*-acylbenzamidoxime (Scheme 2). In spite of the fairly low yield (25%), the protocol was very effective as the resulting **BOxAzaPy** crystallised from the crude with high purity.

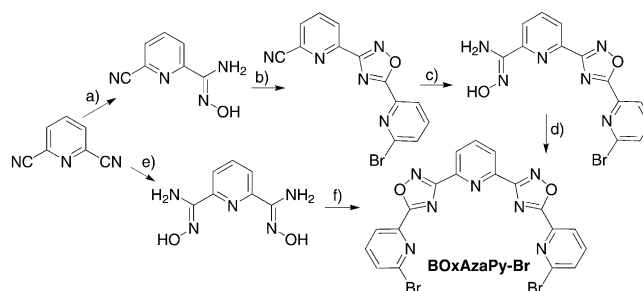


Scheme 2. Synthesis of the prototype **BOxAzaPy**: a) CDI, DMF, 30 min, room temperature; b) 12 h,  $T = 150^\circ\text{C}$  (25%; yield).

**Stepwise synthesis of the precursor for the water soluble BOxAzaPy compounds:** As a first attempt, a very similar one-pot strategy was followed for the synthesis of the bromo analogue **BOxAzaPy-Br** starting from *N*<sup>2</sup>,*N*<sup>6</sup>-dihydroxypyridine-2,6-bis(carboximidamide) and 6-bromopyridine-2-carboxylic acid (Scheme 3).

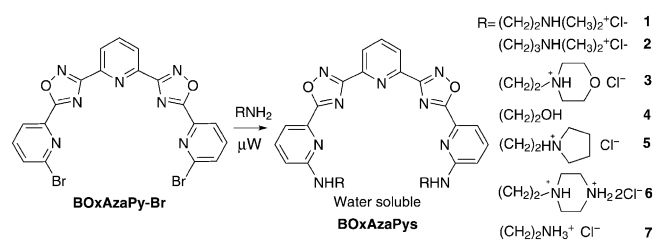
Unfortunately, such a direct approach yielded the **BOxAzaPy-Br** as by-product in a sloppy mixture with very low yield (<3%). A much better result was achieved with a stepwise synthesis, by performing the *O*-acylation and the cyclodehydration to the oxadiazole moieties in two sequential steps (Scheme 3, b and d).

**Solvent-free microwave-assisted synthesis of the water soluble BOxAzaPy compounds (series I):** In order to improve water solubility, we specifically desired access to a diverse



Scheme 3. Stepwise and one-pot synthesis of **BOxAzaPy-Br**. a) 1 equiv  $\text{NH}_2\text{OH}\cdot\text{HCl}$ ,  $\text{Na}_2\text{CO}_3$ ,  $\text{EtOH}/\text{H}_2\text{O}$  2:1, room temperature, 1 h; b) CDI, DMF, 30 min, room temperature; 12 h,  $T = 150^\circ\text{C}$ ; c) identical to step a; d) cyclodehydration, see step b; e) 2.2 equiv  $\text{NH}_2\text{OH}\cdot\text{HCl}$ ,  $\text{Na}_2\text{CO}_3$ ,  $\text{EtOH}/\text{H}_2\text{O}$  2:1, room temperature, 1 h; f) cyclodehydration, see step b.

set of basic or protic moieties at the C-2 positions on both the terminal pyridines in the prototype **BOxAzaPy** scaffold. Previous reports suggest that aromatic nucleophilic substitution ( $\text{S}_{\text{N}}\text{Ar}$ ) with halo-aromatics, such as 2-fluoropurines with amines, requires a temperature higher than  $100^\circ\text{C}$ , and an extended reaction time (12–24 h). Reaction time could be significantly shortened (15 min) and reaction yields improved following a microwave-assisted protocol in polar aprotic solvents, such as ACN (acetonitrile) or ACN/NMP (*N*-methylpyrrolidinone) mixture.<sup>[9]</sup> In order to define the best synthetic protocol for the  $\text{S}_{\text{N}}\text{Ar}$  reactions on the **BOxAzaPy-Br** (Scheme 4), we carried out a comparative evalua-



Scheme 4. Synthesis of water soluble **BOxAzaPy** compounds (series I) by a solvent-free and microwave-assisted aromatic nucleophilic substitution ( $\text{S}_{\text{N}}\text{Ar}$ ).

tion of the thermal and the microwaved reactions in both DMF and in neat amine for compound **1**. Poor conversions were observed with both DMF as solvent and neat amine coupled with the thermal treatment. The results summarised in Table 1 unambiguously suggest the solvent-free microwave-assisted approach as the most effective. Therefore, this synthetic method was extended to an array of primary amines (Table 1). The resulting water soluble **BOxAzaPy** compounds were purified by preparative HPLC (gradient ACN/ $\text{H}_2\text{O}$ ; 0.1%  $\text{CF}_3\text{COOH}$ ), subsequently exchanging the trifluoroacetate with chloride anion, to yield the **BOxAzaPy** compounds as hydrochlorides **1–7** (Table 1).

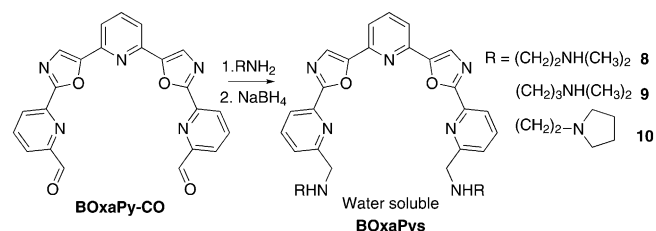
**Synthesis of cationic BOxApys (series II):** In order to investigate the full potential of these polyheterocyclic structures, and to compare their activity as G4 binders as a function of

Table 1. Reactivity of several amines with **BOxAzaPy-Br**.

<b>BOxAzaPy</b>	Amines	Conditions <sup>[a]</sup>	Yields [%] <sup>[b]</sup>	Yields [%] <sup>[c]</sup>
<b>1</b>		$\mu$ W, neat amine	21.4	27.8
		$\mu$ W, DMF	–	$\leq 2$
		$\Delta$ , neat amine	–	11.0
		$\Delta$ , DMF	–	6.3
<b>2</b>		$\mu$ W, neat amine	24.6	53.3
<b>3</b>		$\mu$ W, neat amine	28.7	54.4
<b>4</b>		$\mu$ W, neat amine	46.5	56.8
<b>5</b>		$\mu$ W, neat amine	27.7	51.4
<b>6</b>		$\mu$ W, neat amine	21.9	66.7
<b>7</b>		$\mu$ W, neat amine	22.6	47.6

[a] Microwave ( $\mu$ W), standard conditions in 5 mL microwave vials: amine (2 mL) in the presence of **BOxAzaPy-Br** (100 mg, 0.19 mmol), microwaved 8 min at  $T=100^\circ\text{C}$ ,  $P=462$  kPa;  $\Delta$ , standard conditions in 2 mL of amine or DMF (with 2 equiv amine), 24 h at  $T=100^\circ\text{C}$ . [b] Yields measured on the basis of isolated products by preparative HPLC, followed by trifluoroacetate/chloride anion exchange. [c] Yields measured on the basis of HPLC integration.

the nature of the five-member heterocycle, water soluble **BOxApy** derivatives were synthesised. The already described dialdehyde precursor **BOxApy-CO** (Scheme 5)<sup>[7]</sup> was trans-

Scheme 5. Synthesis of **BOxApy** analogues **8–10** (series II).

formed into the symmetric bisamines (**8–10**) by a one-pot reductive amination, in the presence of  $\text{NaBH}_4$  in absolute ethanol (Scheme 5). Compounds **8–10** were purified by silica gel chromatography ( $\text{CH}_2\text{Cl}_2/\text{MeOH}$  9:1,  $\text{NH}_3$  0.1 %; see the Supporting Information).

**FRET-melting assays:** Stabilisation of the telomeric sequence by the **BOxAzaPy** and the **BOxApy** series was first investigated with FRET-melting assays (Figure 1).<sup>[10]</sup> Compounds **1**, **2** and **5** were found to be potent stabilisers of F21T in potassium-rich buffer ( $\Delta T_{1/2} = +15.5$ ,  $10.5$  and  $16.0^\circ\text{C}$ , for **1**, **2** and **5**, respectively). Their stabilising effect was significantly lessened in sodium-rich buffer ( $+5.2$ ,  $5.5$ ,  $7.0^\circ\text{C}$ , respectively); this suggests a marked structure preference for the  $\text{K}^+$  forms. This trend is not unexpected and has been observed for most classes of quadruplex ligands, however, it is more pronounced in the present case.<sup>[7]</sup> On the other hand, this selectivity is inverted compared to that of

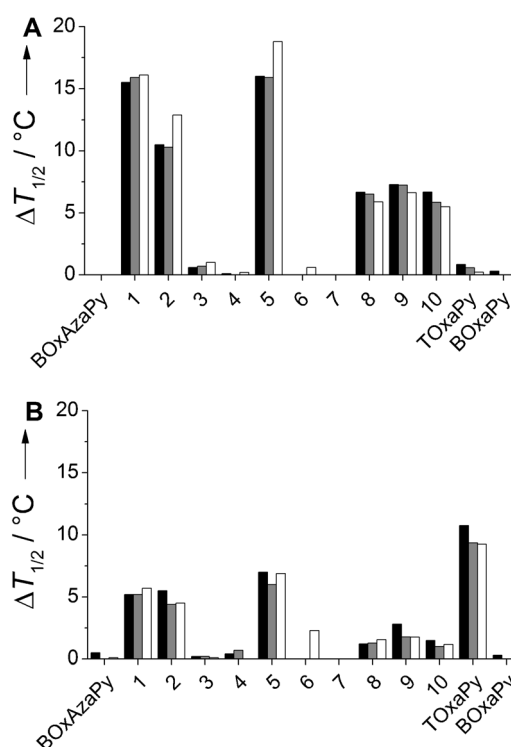


Figure 1. Quantitative analysis of the FRET-melting competition experiments with the telomeric sequence F21T. Stabilisation in: A)  $\text{K}^+$ , or B)  $\text{Na}^+$  is indicated for the prototype **BOxAzaPy**, **1–10**, and the references **TOxApy** and **BOxApy** in the absence (black bars) or presence of double-stranded DNA (ds26) at  $3 \mu\text{M}$  (grey bars) or  $10 \mu\text{M}$  (white bars).

the heptyl **TOxApy** (Figure 1), which bound the telomeric quadruplex much better in  $\text{Na}^+$ .<sup>[7]</sup> However, the latter is neutral and has two more oxazole units. Strikingly, all the other compounds of the **BOxAzaPy** series were inactive ( $\Delta T_{1/2} < +1.0^\circ\text{C}$ ), despite exhibiting the same scaffold. Thus, the nature of the chain clearly is a prominent structural feature in the binding of the series.

The lack of both side chains in the prototype **BOxAzaPy** and fully protonated ending groups (**3** and **4**) at the experimental pH, resulted in a negligible stabilisation. This may be the result of a lower solubility and a deficiency in electrostatic interactions with the quadruplex phosphate backbone.<sup>[11]</sup> This observation is fully consistent with our previous results showing that the deaza analogue **BOxApy**, is unable to stabilise the human telomeric quadruplex.<sup>[7]</sup> In addition, the importance of the terminal amino group has already been described in the case of acridine derivatives and it was shown that larger ring substituents, like piperidines or piperazine, deteriorate the affinity for quadruplexes.<sup>[11a, 12]</sup> This trend may explain the complete absence of binding of **6**, which still represents a striking result. The best solubilising groups for the **BOxAzaPy** series are therefore basic pyrrolidine and dimethylamine, as already observed for other scaffolds.<sup>[12b, c, 13]</sup> The length of the chain was also important, as **1** is a better stabiliser than **2**, perhaps because the terminal ammonium has a better target accessibility.<sup>[14]</sup>

Importantly, the best ligands **1**, **2** and **5**, as well as **8–10**, fully retained their stabilising properties when an excess of duplex DNA competitor was added, irrespective of the chain length, ending group nature, and buffer (potassium- or sodium-rich buffer). This is even more remarkable as the quadruplex stabilising effect is absolutely not affected by the duplex competitor; this indicates that the three ligands are completely devoid of affinity for the double-stranded form under these conditions. Concerning the three derivatives of series II (**8–10**), they exhibit the same trends, but appear clearly less efficient. As they bear the same side chains as **1**, **2** and **5** (differing only by one CH<sub>2</sub>), these data evidence the advantage of the **BOxAzaPy** scaffold. The rest of the study was thus more focused on compounds **1**, **2** and **5**. The latter were studied more comprehensively with a set of quadruplex-forming sequences (DNA and RNA human telomeric sequences 21AG and 21RNAG, modified human telomeric sequence 21CTA, human minisatellite sequence 25Ceb, proto-oncogenes *c-myc*, *c-kit1* and *c-kit2*) and a duplex-forming sequence, dx (for sequences see the Experimental Section). Similar trends were observed for the three ligands. In more detail, 21AG, 21CTA, *c-kit1* and *c-kit2* were the least stabilised structures in sodium-rich buffer, whereas the difference with other sequences was significantly lower or inexistent in potassium-rich conditions (Figure 2). Sequences 21RNAG, 25Ceb and *c-myc* seem to be stabilised in a comparable way in both conditions. Moreover, the duplex sequence (dx) was not stabilised, regardless of the ligand or the cation; this is in accord with the competitive FRET-melting results. Overall, these results suggest that the binding of **BOxAzaPy** ligands is controlled by the quadruplex nucleic acid structure, rather than by the cation nature itself. Moreover, the data demonstrate that duplex matrices offer no binding sites for the new ligands in spite of their dicationic charge.

**High-throughput fluorescent intercalator displacement (HT-G4-FID) assays:** The ligands' affinity for quadruplex and duplex oligonucleotides were tested by HT-G4-FID.<sup>[15]</sup> Briefly, the assay is based on the competitive displacement of the fluorescent probe TO (thiazole orange), which binds various nucleic acid structures. A variety of G-quadruplex structures (*c-myc*, *c-kit1*, *c-kit2*, 21CTA, TBA and 22AG in potassium- or sodium-rich buffers, called 22AG.K and 22AG.Na, respectively, hereafter) and one control duplex matrix, ds26, were used. The **BOxAzaPy** compounds **1**, **2** and **5** and the **BOxApy** derivative **10** appeared to interact preferentially with the telomeric sequence in potassium-rich buffer, whereas a very weak interaction was observed in sodium-rich buffer (Figure 3, for selected results) thus paralleling the FRET-melting data. The **BOxApy** compounds **9–10** exhibited a systematic lower affinity and a poor selectivity toward different quadruplexes (22AG.K, 22AG.Na, 21CTA, *c-myc*, *c-kit1*, *c-kit2*, TBA, see Figure S1 in Supporting Information for full data). Therefore, the **BOxapy** series was discarded for further experiments.

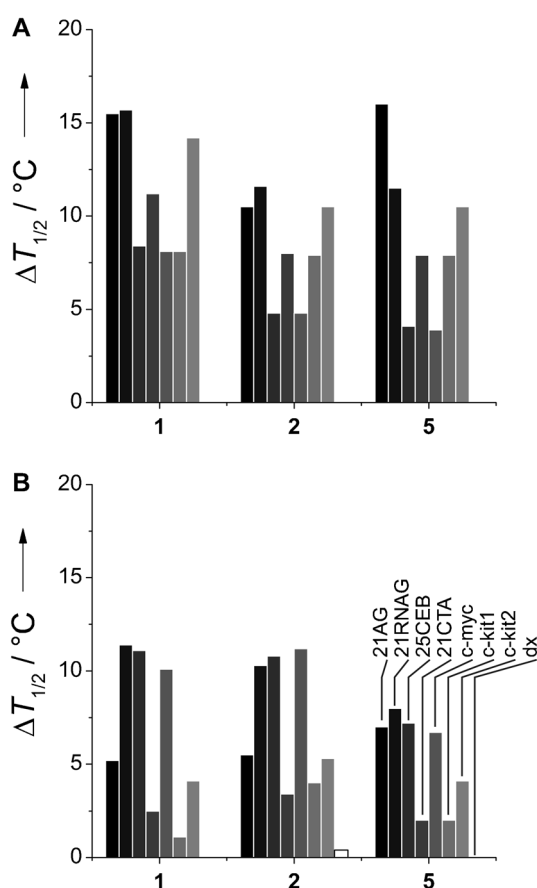


Figure 2. FRET-melting stabilisation by derivatives **1**, **2** and **5** ( $\Delta T_{1/2}$ , °C) of the quadruplexes 21AG, 21RNAG, 25Ceb, 21CTA, *c-myc*, *c-kit1*, *c-kit2* and of the duplex dx in: A) K<sup>+</sup>-, or B) Na<sup>+</sup>-rich buffers. [DNA] = 0.2  $\mu$ M; [ligands] = 1  $\mu$ M.

Generally, **1** appeared significantly more efficient than all other compounds with regard to the set of quadruplexes investigated. Such a difference in behaviour is remarkable as the three ligands have very close structures; in particular **1** differs from **2** only by one CH<sub>2</sub> group in the side chains. However, although more active than **2** and **5**, **1** displays a moderate ability to displace TO as compared to the planar ligand **Pt-ttpy** {[Pt(4'-(4-methylphenyl)-2,2':6',2''-terpyridine)Cl]Cl} used as benchmark (Figure 3 A and B).<sup>[16]</sup> Indeed, the displacement curves never reach saturation (the probe being displaced by up to 60–80% in the best cases), and the shape of the curve is irregular, thereby reflecting a slow and/or complex process. This type of curve may reflect either a poor affinity for the TO sites, or an indirect competition between TO and the ligand due to different binding sites. In addition, conformational changes of the G4 target that in turn may modify the TO/G4 equilibrium cannot be excluded.<sup>[7]</sup> Finally, the FID data unambiguously confirm the absence of binding to duplex structures (Figure 3D). The high and structurally selective stabilisation properties of these compounds, together with their moderate TO displacing properties, suggest a binding mode different from the usual  $\pi$  stacking on external quartets. It is likely that com-

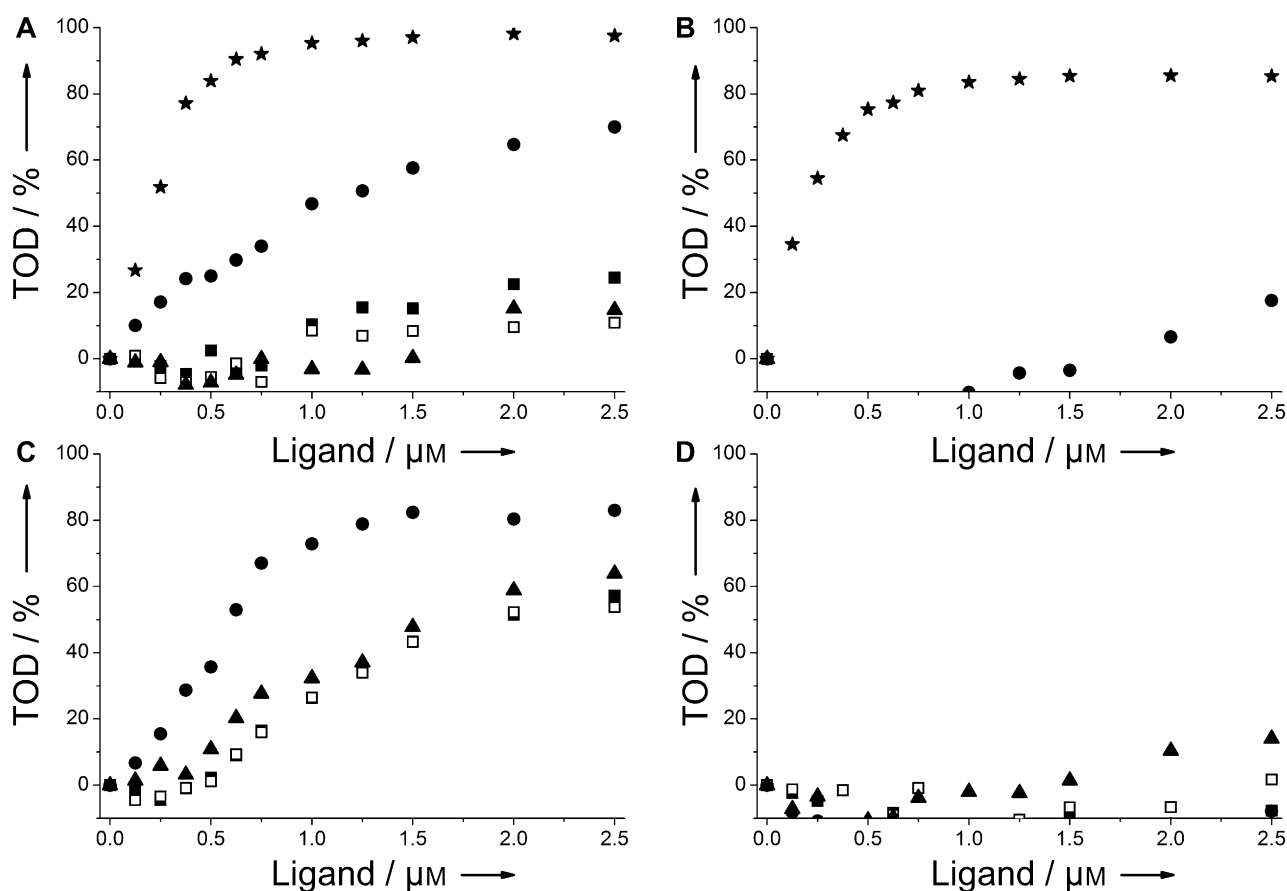


Figure 3. G4-FID plots of **1** (●), **2** (■), **5** (□) and **10** (▲) with: A) 22AG.K, B) 22AG.Na, C) *c-myc*, and D) ds26. **Pt-ttpty** (&ssstarf, A and B) is used as a benchmark as it is a strong TO displacer for these G4 structures and has a stabilising effect in a comparable range (15°C).

compound **1**, due to its flexible and non-planar structure, is well-suited to interact with loops and grooves. Interestingly, a similar behaviour (strong G4 stabilisation, partial displacement of TO, discrimination between various G4 matrices, no duplex binding) has been observed for the structurally related heptaryl **TOxaPy**,<sup>[7]</sup> for which molecular modelling studies supported the possibility of interaction in the grooves. It might well be that these polyheteroaryl series make use of a groove-binding mode or of mixed binding modes (loop-quartet, groove-quartet) to achieve recognition of quadruplex matrices, as already reported for the ribbon-like distamycin derivatives.<sup>[17]</sup> Finally, we noticed again that the FID assay emphasises differences between ligands that are not detected by FRET melting (compare **1** and **5**) and thus the two assays nicely complement each other to give a more complete picture of the ligand-binding profile.

**Circular dichroism (CD) spectroscopy:** In an attempt to gain insight into the interaction of **BoxAzaPy** ligands with G4-DNA, we conducted CD experiments. We first verified that the achiral compound **1** did not display any CD signal in its absorbance region (Figure S2 in the Supporting Information). The spectrum of the prefolded human telomeric sequence, 22AG, in potassium-rich buffer was consistent with results reported in the literature for the same sequence at

submillimolar nucleoside concentration, that is, a maximum at 290 nm (usually observed with antiparallel strands), a shoulder around 265 nm and a minimum at 240 nm (both observed with parallel strands; Figure 4A).<sup>[18]</sup>

This spectrum may correspond to an antiparallel basket arrangement,<sup>[18c]</sup> (3+1) hybrid structures<sup>[18b]</sup> or a mixture of parallel and antiparallel structures.<sup>[18b,19]</sup> Secondary structures of the telomeric sequence, and corresponding CD spectra, are very concentration dependent in potassium-rich buffers: high concentrations result in (3+1) hybrid structures as observed with NMR spectroscopy,<sup>[18c,20]</sup> whereas an antiparallel basket arrangement seems to be favoured at low concentrations.<sup>[18c]</sup> Upon addition of **1**, a strong increase of the 290 nm band, together with the conversion of the positive shoulders to a negative band at 260 nm, was observed (Figure 4A), suggesting a **1**-22AG.K complex formation. This non-conservative positive exciton couplet signature is characteristic of an antiparallel structure, and its induction by ligands like sanguinarine<sup>[21]</sup> or telomestatin<sup>[5b]</sup> has already been observed. The presence of two neat isoelectronic points at 285 and 245 nm supports the existence of a single equilibrium converting the free DNA structure(s) into a bound species.

An apparent 2:1 stoichiometry can be inferred by plotting the variation of intensity of the 290 and 260 nm bands as a

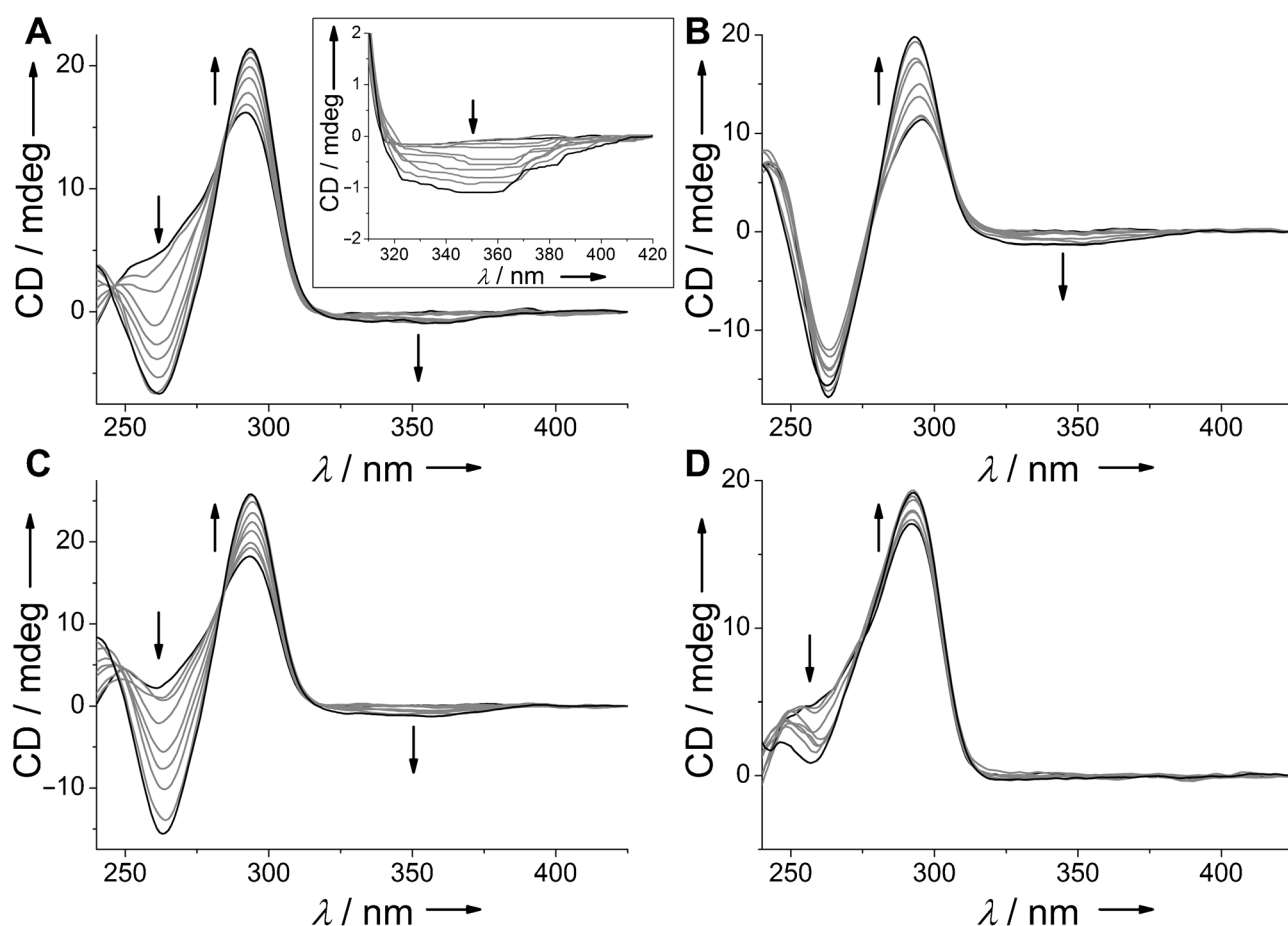


Figure 4. CD spectra of 22AG alone and upon addition of increasing amounts of **1** (indicated by the arrows; A, B and C) or **5** (D) in potassium-rich buffer (A, D), sodium-rich buffer (B) or in the absence of salts (C). Inset A: magnification of the 310–420 nm region, corresponding to an induced CD of the achiral ligand **1**.

function of **1** concentration (Figure S3 A in the Supporting Information). Global fitting by using nonlinear regression of both scatter plots with the Hill equation, with shared binding and Hill constants, was successfully achieved, and yielded a shared apparent dissociation constant  $K_d = 5.3(\pm 0.3) \times 10^{-6} \text{ M}$  (Figure S3 B in the Supporting Information). Since DNA does not absorb above 320 nm, the change in ellipticity monitored in the 320–400 nm region has to be assigned to induced CD (ICD) of the achiral ligand, as a result of **1** sensing the quadruplex chirality in the complex (Figure 4 A, insets). ICD was also observed for compound **1** with two quadruplex-forming sequences the G4 structures of which are not cation dependent: namely the tetramolecular quadruplex  $[5'\text{-TG4T-3}']_4$  and *c-myc* (data not shown). The same experiment was carried out in sodium-rich buffer. The telomeric antiparallel structure is characterised by positive bands at 245 and 290 nm and a negative band at 260 nm (Figure 4 B and Figure S4 A in the Supporting Information, dark blue line).<sup>[18b,22]</sup> Upon addition of **1**, a strong increase of the 290 nm band was recorded, together with a 3 nm hypsochromic shift. The first two equivalents of ligand induced a decrease of the intensity of the 260 nm band, but higher ligand concentrations almost restored the initial ellipticity

value (Figure S4 B in the Supporting Information). There is no clear isoelliptic point; therefore, we can infer that the spectrum obtained by the addition of two equivalents of **1** may arise from an intermediate structure or the coexistence of more than two bound structures.

Finally, the interaction between 22AG and **1** was studied in the absence of cations (Figure 4 C and Figure S5 A in the Supporting Information), as already described.<sup>[5b]</sup> Results obtained with the oligonucleotide prepared in the absence of monovalent cations are very similar to the ones obtained in potassium-rich buffer, that is: 1) an increase of the 290 nm band, 2) the formation of a negative ellipticity band at 260 nm, 3) the presence of an isoelliptic point at 285 nm, and 4) the appearance of an ICD band. We can thus conclude that **1** binds to the telomeric sequence and preferentially induces a single antiparallel structure, which seems similar to the one obtained by complexation of (*R*)- or (*S*)-telomestatin.<sup>[5b]</sup> Global fitting was also achieved successfully and shows a comparable dissociation constant ( $K_d = 1.1(\pm 0.1) \times 10^{-6} \text{ M}$ ) to the one obtained in potassium-rich buffer (Figure S6 B in the Supporting Information). Interestingly, the spectra obtained after complexation of **1** to the randomly structured (absence of metallic salt) or the prefolded telo-

meric sequence in sodium or potassium converged to an analogous pattern, although they differ greatly in the free-state (Figure S6 in the Supporting Information).

In order to gain additional insight into the SAR (structure–activity relationship) of the **BOxAzaPy** series, we also investigated the behaviour of **5** with the telomeric sequence in potassium- or sodium-rich buffer (Figure 4D and Figure S6 in the Supporting Information). The trends were the same as those already monitored for **1**, in the DNA absorbing region, but to a significantly lesser extent. Thus, in potassium-rich conditions, the 290 nm band intensity increases moderately and a 260 nm negative band only begins to appear. In sodium-rich conditions, the 260 nm band grows but the 290 nm band remains unchanged. Compared to **1**, **5** seems to induce the formation of a similar antiparallel structure (Figure S6 in the Supporting Information, dashed lines vs. solid lines) regardless of the cation nature, but is a poorer inducer. Finally, it is worth noting that no ICD is detectable in the 320–400 nm region for **5** (Figure 4D and Figure S6 in the Supporting Information). This might result from a slightly different binding interaction both in terms of affinity and structure, which would be consistent with the different FID behaviour exhibited by the two compounds.

## Conclusion

Using a microwave-assisted solvent-free synthetic protocol we have created and investigated a new family of water soluble oxadiazole-based acyclic quadruplex ligands. The promising binding properties of three of these ligands (**1**, **2** and **5**) together with the selectivity toward both quadruplex versus duplex and within different G-quadruplexes have been highlighted by FRET melting, HT-G4-FID and circular dichroism experiments. Our data reveal the unexpected potential of these acyclic derivatives. In fact, the on/off quadruplex binding properties are clearly controlled by the structural features of the cationic moieties and optimised by the oxadiazole core, as the oxazole analogues are much less efficient G4 ligands. The sharp structure–activity relationships, the conformational flexibility and the highly hydrophobic character of the pentameric core are in favour of specific interactions that may be established in the grooves of the quadruplex, at least for ligand **1**, as it exhibited ICD. However, a thorough structural investigation is needed to unambiguously confirm the proposed binding mode.

## Experimental Section

**Synthesis of 2,6-bis(5-(pyridin-2-yl)-1,2,4-oxadiazol-3-yl)pyridine (BOxAzaPy):** Pyridine-2,6-dicarboxylic acid (0.35 g, 2.8 mmol) and 1,1'-carbonyldiimidazole (CDI, 0.46 g, 2.8 mmol) were dissolved in DMF (14 mL) and stirred at room temperature for 30 min. (2*Z*,6*Z*)-*N*'<sup>2</sup>,*N*'<sup>6</sup>-Dihydroxypyridine-2,6-bis(carboximidamide)<sup>[23]</sup> (0.25 g, 1.28 mmol) was added and the reaction mixture was stirred at room temperature, overnight. CDI (0.46 g, 2.8 mmol) was further added and the reaction mixture was heated at 150°C for 6 h. After being cooled, the reaction mixture was

poured into water to induce the precipitation of a white solid (0.12 g; yield 25%), which was filtered and characterised as pure product; m.p. > 300°C (dec.); <sup>1</sup>H NMR (300 MHz, [D<sub>6</sub>]DMSO, 25°C, TMS): δ = 8.92–8.89 (m, 2H), 8.48–8.45 (m, 4H), 8.12 (t, <sup>3</sup>J(H,H) = 8 Hz, 1H), 8.02–7.96 (dt, <sup>3</sup>J(H,H) = 8 Hz; <sup>4</sup>J(H,H) = 2 Hz, 2H), 7.61–7.56 ppm (ddd, <sup>3</sup>J(H,H) = 6 Hz; <sup>3</sup>J(H,H) = 5 Hz; <sup>4</sup>J(H,H) = 2 Hz, 2H); <sup>13</sup>C NMR (75 MHz, [D<sub>6</sub>]DMSO, 25°C, TMS): δ = 175.1, 168.3, 150.6, 146.9, 143.3, 138.3, 137.3, 126.8, 125.2, 124.6 ppm; elemental analysis calcd (%) for C<sub>19</sub>H<sub>11</sub>N<sub>7</sub>O<sub>2</sub>: C 61.79, H 3.00, N 26.55; found: C 61.64, H 3.01, N 26.48.

**Stepwise synthesis of BOxAzaPy-Br:** The experimental details refer to steps a)–d) in Scheme 3.

a) *6-Cyano-N-hydroxy-pyridine-2-carboxamide*:<sup>[24]</sup> Hydroxylamine hydrochloride (0.53 g, 7.7 mmol) and Na<sub>2</sub>CO<sub>3</sub> (0.41 g, 3.9 mmol) in water (50 mL) were added dropwise to a solution containing pyridine-2,6-dicarbonitrile<sup>[24]</sup> (1.00 g, 7.7 mmol) dissolved in EtOH (100 mL). The reaction mixture was stirred at room temperature for 1 h. The organic solvent was removed and the white solid was filtered and washed with water. The crude product was purified by MPLC (Isolera ONE; eluent CHCl<sub>3</sub>/MeOH gradient) and the product (*Z*)-6-cyano-*N*-hydroxy-pyridine-2-carboxamide was obtained as a white pale solid (0.52 g; yield 41%) and used for the next step without further purification. <sup>1</sup>H NMR (300 MHz, [D<sub>6</sub>]DMSO, 25°C, TMS): δ = 10.25 (s, 1H), 8.15–8.11 (m, 1H), 8.07–8.04 (m, 2H), 5.93 ppm (s, 1H); <sup>13</sup>C NMR (75 MHz, [D<sub>6</sub>]DMSO, 25°C, TMS): δ = 151.8, 148.4, 138.3, 131.2, 129.3, 123.6, 117.3 ppm.

b) *6-[5-(6-Bromopyridin-2-yl)-[1,2,4]oxadiazol-3-yl]-pyridine-2-carbonitrile*: 6-Bromopyridine-2-carboxylic acid (0.33 g, 1.6 mmol) and CDI (0.26 g, 1.6 mmol) were dissolved in DMF (8 mL) and stirred at room temperature for 30 min. Then, (*Z*)-6-cyano-*N*'-hydroxypicolinimidamide (0.26 g, 1.6 mmol) was added and the reaction mixture was stirred at room temperature, overnight. CDI (0.26 g, 1.6 mmol) was further added and the reaction mixture was refluxed for 6 h. After being cooled, the reaction mixture was poured into water to induce the precipitation of the white solid (0.16 g, yield 59%), which was filtered and used without purification; m.p. 270–272°C; <sup>1</sup>H NMR (300 MHz, [D<sub>6</sub>]DMSO, 25°C, TMS): δ = 8.48 (d, <sup>3</sup>J(H,H) = 8 Hz, 1H), 8.38 (t, <sup>3</sup>J(H,H) = 8 Hz, 1H), 8.32 (d, <sup>3</sup>J(H,H) = 8 Hz, 1H), 8.24 (d, <sup>3</sup>J(H,H) = 8 Hz, 1H), 8.09 (t, <sup>3</sup>J(H,H) = 8 Hz, 1H), 7.99 ppm (d, <sup>3</sup>J(H,H) = 8 Hz, 1H); <sup>13</sup>C NMR (75 MHz, [D<sub>6</sub>]DMSO, 25°C, TMS): δ = 173.9, 167.5, 146.9, 143.2, 141.9, 141.1, 139.9, 133.4, 132.1, 130.9, 127.1, 124.1, 116.7 ppm.

c) *6-[5-(6-Bromopyridin-2-yl)-[1,2,4]oxadiazol-3-yl]-N-hydroxy-pyridine-2-carboxamide*: A mixture of hydroxylamine hydrochloride (0.13 g, 1.9 mmol) and of Na<sub>2</sub>CO<sub>3</sub> (0.1 g, 0.9 mmol) in water (25 mL) was added dropwise to a solution containing 6-[5-(6-bromopyridin-2-yl)-[1,2,4]oxadiazol-3-yl]-pyridine-2-carbonitrile (0.3 g, 0.9 mmol) in EtOH (75 mL) and the reaction mixture was stirred at room temperature, overnight. The organic solvent was removed and the solid was filtered, washed with water and dried. The desired product was obtained as a white pale solid (0.25 g, yield 75%), m.p. 225–230°C; <sup>1</sup>H NMR (300 MHz, CDCl<sub>3</sub>, 25°C, TMS): δ = 10.15 (s, 1H), 8.39 (d, <sup>3</sup>J(H,H) = 7 Hz, 1H), 8.19 (t, <sup>3</sup>J(H,H) = 5 Hz, 1H), 8.08–8.05 (m, 3H), 8.01 (d, <sup>3</sup>J(H,H) = 8 Hz, 1H), 5.89 ppm (s, 2H); <sup>13</sup>C NMR (75 MHz, CDCl<sub>3</sub>, 25°C, TMS): δ = 173.4, 168.2, 150.7, 148.8, 144.1, 143.3, 141.9, 141.3, 138.3, 132.1, 124.1, 123.7, 121.9 ppm.

d) *2,6-Bis(5-(6-bromopyridin-2-yl)-1,2,4-oxadiazol-3-yl)pyridine (BOxAzaPy-Br)*: 6-Bromopyridine-2-carboxylic acid (0.18 g, 0.9 mmol) and CDI (0.15 g, 0.9 mmol) were dissolved in DMF (5 mL) and stirred at room temperature for 30 min. Then, (*Z*)-6-(5-(6-bromopyridin-2-yl)-1,2,4-oxadiazol-3-yl)-*N*'-hydroxypicolinimidamide (0.28 g, 1.6 mmol) was added and the reaction mixture was stirred at room temperature, overnight. CDI (0.15 g) was further added and the reaction mixture was heated to reflux for 6 h. After being cooled, the reaction mixture was poured into water and the product was filtered as a white solid (0.25 g; 0.47 mmol); m.p. > 300°C (dec.); <sup>1</sup>H NMR (300 MHz, CDCl<sub>3</sub>, 25°C, TMS): δ = 8.62–8.48 (m, 4H), 8.20 (t, <sup>3</sup>J(H,H) = 8 Hz, 1H), 8.02–7.88 ppm (m, 4H); <sup>13</sup>C NMR (75 MHz, CDCl<sub>3</sub>, 25°C, TMS): δ = 173.0, 168.4, 139.4, 138.4, 134.5, 131.9, 130.1, 126.4, 125.4, 123.4 ppm.

**Solvent-free microwave-assisted synthesis of the water soluble BOxAzaPy compounds (1–7): general procedure:** BOxAzaPy-Br (0.1 g, 0.19 mmol) was dissolved in neat amine (2 mL) and the mixture was irra-

diated for 8 min in a closed-vessel microwave oven (power=200 W,  $T_{\max}$ =100°C,  $P_{\max}$ =462 kPa; CEM single-mode microwave reactor). Excess solvent was removed under high vacuum (<7 Pa). The crude product, was dissolved in methanol and purified by preparative HPLC, by using a C-18 reverse phase column (CH<sub>3</sub>CN/H<sub>2</sub>O, 0.1% TFA, as eluent). Addition of HCl solution (1 M; 0.5 mL) to each chromatographic portion and subsequent solvent evaporation under vacuum afforded adducts **1–7**, as hydrochlorides.

Compound **1**: pale yellow crystals; m.p.>300°C; <sup>1</sup>H NMR (300 MHz, [D<sub>6</sub>]DMSO, 25°C, TMS): δ=10.83 (s, 2H), 8.39–8.35 (m, 3H), 7.76 (t, <sup>3</sup>J(H,H)=7 Hz, 2H), 7.59 (d, <sup>3</sup>J(H,H)=6 Hz, 2H), 6.96 (d, <sup>3</sup>J(H,H)=8 Hz, 2H), 3.72 (bs, 4H), 3.36 (bs, 4H), 2.98 ppm (s, 12H); <sup>13</sup>C NMR (75 MHz, [D<sub>6</sub>]DMSO, 25°C, TMS): δ=175.4, 167.0, 158.5, 146.1, 139.8, 139.6, 138.4, 125.7, 114.4, 113.5, 57.1, 42.7, 36.5 ppm; elemental analysis calcd (%) for C<sub>27</sub>H<sub>33</sub>Cl<sub>2</sub>N<sub>11</sub>O<sub>2</sub>: C 52.77, H 5.41, Cl 11.54, N 25.07; found: C 52.67, H 5.46, Cl 11.44, N 24.96.

Compound **2**: pale yellow crystals; m.p.>300°C; <sup>1</sup>H NMR (300 MHz, [D<sub>6</sub>]DMSO, 25°C, TMS): δ=10.54 (s, 2H), 8.42–8.34 (m, 3H), 7.70 (t, <sup>3</sup>J(H,H)=7 Hz, 2H), 7.54 (d, <sup>3</sup>J(H,H)=7 Hz, 2H), 6.88 (d, <sup>3</sup>J(H,H)=8 Hz, 2H), 3.47–3.43 (m, 4H), 3.21–3.14 (m, 4H), 2.81 (s, 12H), 2.07–1.99 ppm (m, 4H); <sup>13</sup>C NMR (75 MHz, [D<sub>6</sub>]DMSO, 25°C, TMS): δ=175.5, 167.9, 158.9, 146.4, 140.2, 139.7, 137.9, 125.6, 113.4, 113.0, 54.5, 42.1, 37.8, 24.0 ppm; elemental analysis calcd (%) for C<sub>29</sub>H<sub>37</sub>Cl<sub>2</sub>N<sub>11</sub>O<sub>2</sub>: C 54.20, H 5.80, Cl 11.03, N 23.98; found: C 53.98, H 5.82, Cl 11.08, N 24.07.

Compound **3**: pale yellow crystals; m.p.>300°C; <sup>1</sup>H NMR (300 MHz, [D<sub>6</sub>]DMSO, 25°C, TMS): δ=11.11 (s, 2H), 8.40–8.34 (m, 3H), 7.74 (t, <sup>3</sup>J(H,H)=8 Hz, 2H), 7.61 (d, <sup>3</sup>J(H,H)=7 Hz, 2H), 6.92 (d, <sup>3</sup>J(H,H)=8 Hz, 2H), 4.00–3.97 (m, 4H), 3.89–3.82 (m, 8H), 3.64 (d, <sup>3</sup>J(H,H)=12 Hz, 4H), 3.38 (d, <sup>3</sup>J(H,H)=4 Hz, 4H), 3.20–3.16 ppm (m, 4H); <sup>13</sup>C NMR (75 MHz, [D<sub>6</sub>]DMSO, 25°C, TMS): δ=175.5, 167.9, 158.4, 146.4, 140.3, 139.6, 138.1, 125.6, 113.8, 113.7, 63.1, 56.0, 55.5, 51.4, 35.1 ppm; elemental analysis calcd (%) for C<sub>31</sub>H<sub>37</sub>Cl<sub>2</sub>N<sub>11</sub>O<sub>4</sub>: C 53.30, H 5.34, Cl 10.15, N 22.05; found: C 53.04, H 5.30, Cl 10.26, N 22.28.

Compound **4**: pale yellow crystals; m.p.>300°C; <sup>1</sup>H NMR (300 MHz, [D<sub>6</sub>]DMSO, 25°C, TMS): δ=8.40–8.33 (m, 3H), 7.67 (t, <sup>3</sup>J(H,H)=7 Hz, 2H), 7.52 (d, <sup>3</sup>J(H,H)=7 Hz, 2H), 6.88 (d, <sup>3</sup>J(H,H)=8 Hz, 2H), 3.63–3.56 (m, 4H), 3.47–3.43 ppm (m, 4H); <sup>13</sup>C NMR (75 MHz, [D<sub>6</sub>]DMSO, 25°C, TMS): δ=175.4, 167.8, 158.9, 146.4, 140.1, 139.6, 137.8, 125.6, 113.2, 112.7, 59.9, 43.5 ppm; elemental analysis calcd (%) for C<sub>23</sub>H<sub>21</sub>N<sub>9</sub>O<sub>4</sub>: C 56.67, H 4.34, N 25.86; found: C 56.84, H 4.32, N 25.81.

Compound **5**: pale yellow crystals; m.p.>300°C; <sup>1</sup>H NMR (300 MHz, [D<sub>6</sub>]DMSO, 25°C, TMS): δ=10.67 (s, 2H), 8.41–8.35 (m, 3H), 7.76 (t, <sup>3</sup>J(H,H)=7 Hz, 2H), 7.62 (d, <sup>3</sup>J(H,H)=7 Hz, 2H), 6.92 (d, <sup>3</sup>J(H,H)=8 Hz, 2H), 3.42–3.38 (m, 4H), 3.17–3.12 (m, 4H), 2.02–1.91 ppm (m, 8H); <sup>13</sup>C NMR (75 MHz, [D<sub>6</sub>]DMSO, 25°C, TMS): δ=175.5, 167.9, 158.5, 146.4, 140.3, 139.6, 138.1, 125.7, 113.9, 113.6, 53.3, 40.3, 38.7, 22.7 ppm; elemental analysis calcd (%) for C<sub>31</sub>H<sub>37</sub>Cl<sub>2</sub>N<sub>11</sub>O<sub>2</sub>: C 55.86, H 5.59, Cl 10.64, N 23.11; found: C 55.51, H 5.62, Cl 10.68, N 23.19.

Compound **6**: pale yellow crystals; m.p.>300°C; <sup>1</sup>H NMR (300 MHz, [D<sub>6</sub>]DMSO, 25°C, TMS): δ=11.75 (s, 2H), 8.63 (s, 4H), 8.55–8.45 (m, 3H), 8.05 (t, <sup>3</sup>J(H,H)=7 Hz, 2H), 7.87 (d, <sup>3</sup>J(H,H)=7 Hz, 2H), 7.48 (d, <sup>3</sup>J(H,H)=8 Hz, 2H), 4.85–4.72 (m, 8H), 3.92–3.83 (m, 4H), 3.57–3.48 (m, 8H), 3.35–3.28 ppm (m, 4H); <sup>13</sup>C NMR (75 MHz, [D<sub>6</sub>]DMSO, 25°C, TMS): δ=175.1, 167.9, 157.9, 146.3, 140.5, 139.6, 139.5, 125.7, 114.8, 112.1, 52.9, 50.9, 41.6, 33.3 ppm; elemental analysis calcd (%) for C<sub>31</sub>H<sub>41</sub>Cl<sub>4</sub>N<sub>13</sub>O<sub>2</sub>: C 48.38, H 5.37, Cl 18.43, N 23.66; found: C 48.43, H 5.40, Cl 18.55, N 23.82.

Compound **7**: pale yellow crystals; m.p.>300°C; <sup>1</sup>H NMR (300 MHz, [D<sub>6</sub>]DMSO, 25°C, TMS): δ=11.14 (s, 2H), 7.96–7.87 (m, 3H), 8.24 (s, 4H), 7.71 (t, <sup>3</sup>J(H,H)=7 Hz, 2H), 7.58 (d, <sup>3</sup>J(H,H)=7 Hz, 2H), 6.89 (d, <sup>3</sup>J(H,H)=8 Hz, 2H), 3.63–3.59 (m, 4H), 3.09–3.00 ppm (m, 4H); <sup>13</sup>C NMR (75 MHz, [D<sub>6</sub>]DMSO, 25°C, TMS): δ=175.5, 167.8, 158.7, 146.4, 140.3, 139.6, 137.9, 125.7, 113.8, 113.5, 41.2, 38.5 ppm; elemental analysis calcd (%) for C<sub>23</sub>H<sub>25</sub>Cl<sub>2</sub>N<sub>11</sub>O<sub>2</sub>: C 49.47, H 4.51, Cl 12.70, N 27.59; found: C 49.33, H 4.53, Cl 12.62, N 27.65.

**Synthesis of BOxaPy derivatives by reductive amination (8–10): general procedure:** BOxaPy-CO (100 mg, 0.236 mmol) was dissolved in absolute

ethanol (5 mL) and the desired amine (**8–10**; 0.709 mmol) was added under nitrogen atmosphere. The reaction mixture was stirred at room temperature for 24 h. NaBH<sub>4</sub> (80.5 mg, 2.13 mmol) was added in one portion. The solution was stirred for another 6 h until the composition of the reaction mixture no longer changed. The solution was concentrated under reduced pressure and to the residue was mixed with water (20 mL). The aqueous solution was extracted with CHCl<sub>3</sub> (3×50 mL). The combined organic phase was dried over Na<sub>2</sub>SO<sub>4</sub> and the solvent was removed under reduced pressure. The obtained reaction mixture was purified by column chromatography CH<sub>2</sub>Cl<sub>2</sub>/MeOH 9:1 with NH<sub>3</sub> (1%). The product was obtained as a pale yellow oil.

*N1,N1'-(6,6'-(5,5'-(Pyridine-2,6-diyl)bis(oxazole-5,2-diyl))bis(pyridine-6,2-diyl))bis(methylene)bis(N2,N2-dimethylethane-1,2-diamine) (8)*: Pale yellow oil (32.8 mg, 23.0% yield); <sup>1</sup>H NMR (300 MHz, CDCl<sub>3</sub>, 25°C, TMS): δ=8.10 (d, <sup>3</sup>J(H,H)=9 Hz, 2H), 7.99 (s, 2H), 7.81–7.94 (m, 5H), 7.52 (d, <sup>3</sup>J(H,H)=9 Hz, 2H), 4.10 (s, 4H), 2.81 (t, <sup>3</sup>J(H,H)=6 Hz, 4H), 2.51 (t, <sup>3</sup>J(H,H)=6 Hz, 4H), 2.29 ppm (s, 12H); <sup>13</sup>C NMR (75 MHz, CDCl<sub>3</sub>, 25°C, TMS): δ=160.9, 151.3, 147.3, 145.3, 137.9, 137.4, 127.9, 123.6, 120.8, 118.9, 59.1, 55.1, 46.9, 45.5 ppm; *m/z* (%): 590 (100) [M<sup>+</sup>+Na<sup>+</sup>], 568 (26) [M<sup>+</sup>], 295 (81.6) [(M<sup>+</sup>+Na<sup>+</sup>)/2]; HRMS (ESI-MS): *m/z* (%): 568.3141; calcd for C<sub>31</sub>H<sub>38</sub>N<sub>9</sub>O<sub>2</sub>: 568.3148.

*N1,N1'-(6,6'-(5,5'-(Pyridine-2,6-diyl)bis(oxazole-5,2-diyl))bis(pyridine-6,2-diyl))bis(methylene)bis(N3,N3-dimethylpropane-1,3-diamine) (9)*: Pale yellow oil (30.0 mg, 21.3% yield); <sup>1</sup>H NMR (300 MHz, CDCl<sub>3</sub>, 25°C, TMS): δ=8.12 (d, <sup>3</sup>J(H,H)=9 Hz, 2H), 8.0 (s, 2H), 7.94–7.82 (m, 5H), 7.50 (d, <sup>3</sup>J(H,H)=9 Hz, 2H), 4.09 (s, 4H), 2.82 (t, <sup>3</sup>J(H,H)=6 Hz, 4H), 2.44 (t, <sup>3</sup>J(H,H)=6 Hz, 4H), 2.28 (s, 12H), 1.80 ppm (m, <sup>3</sup>J(H,H)=6 Hz, 4H); <sup>13</sup>C NMR (75 MHz, CDCl<sub>3</sub>, 25°C, TMS): δ=160.4, 160.7, 151.4, 147.3, 145.4, 138.0, 137.5, 127.9, 123.7, 120.9, 119.0, 56.0, 55.1, 51.5, 48.1, 45.5 ppm; *m/z* (%): 618 (41.5) [M<sup>+</sup>], 596 (100) [M<sup>+</sup>+Na<sup>+</sup>]; HRMS (ESI-MS): *m/z* (%): 596.3450; calcd for C<sub>33</sub>H<sub>42</sub>N<sub>9</sub>O<sub>2</sub>: 596.3461.

*N1,N1'-(6,6'-(5,5'-(Pyridine-2,6-diyl)bis(oxazole-5,2-diyl))bis(pyridine-6,2-diyl))bis(methylene)bis(2-(pyrrolidin-1-yl)ethanamine) (10)*: Pale yellow oil (54.7 mg, 37.4% yield); <sup>1</sup>H NMR (300 MHz, CDCl<sub>3</sub>, 25°C, TMS): δ=8.06 (d, <sup>3</sup>J(H,H)=9 Hz, 2H), 7.96 (s, 2H), 7.77–7.89 (m, 5H), 7.50 (d, <sup>3</sup>J(H,H)=8 Hz, 2H), 4.07 (s, 4H), 2.85 (t, <sup>3</sup>J(H,H)=6 Hz, 4H), 2.70 (t, <sup>3</sup>J(H,H)=6 Hz, 4H), 2.54–2.58 (m, 8H), 1.75–1.79 ppm (m, 8H); <sup>13</sup>C NMR (75 MHz, CDCl<sub>3</sub>, 25°C, TMS): δ=161.0, 160.9, 151.3, 147.2, 145.3, 137.8, 137.4, 127.9, 123.6, 120.8, 118.9, 56.0, 55.2, 54.2, 48.0, 23.4 ppm; *m/z* (%): 642 (44.6) [M<sup>+</sup>+Na<sup>+</sup>], 620 (100.0) [M<sup>+</sup>]; HRMS (ESI-MS): *m/z* (%): 620.3467; calcd for C<sub>35</sub>H<sub>42</sub>N<sub>9</sub>O<sub>2</sub>: 620.3461.

**FRET-melting experiments:** FRET-melting measurements were performed as described previously.<sup>[10]</sup> Experiments were carried out in 96-well plates on a real-time PCR apparatus M×3005P Stratagene as follow: 5 min at 25°C, then increase of 1°C every minute until 95°C. Each experimental condition was tested in duplicate, in a volume of 25 μL for each sample. Oligonucleotides (see below), equipped with FRET partners at each extremity, were prepared at 0.2 μM, ligands were at 1 μM and competitors at 3 or 10 μM final concentration. Measurements were made with excitation at 492 nm and detection at 516 nm in a buffer of lithium cacodylate (10 mM, pH 7.2), NaCl (100 mM) or KCl (10 mM; completed by 90 mM LiCl) then heated at 90°C for 2 min and finally put in ice. The sequences are:

F21T: FAM-G<sub>3</sub>[T<sub>2</sub>AG<sub>3</sub>]<sub>3</sub>-Tamra

FmycT: FAM-T<sub>2</sub>GAG<sub>3</sub>TG<sub>3</sub>TAG<sub>3</sub>TG<sub>3</sub>TA<sub>2</sub>-Tamra

FKit1T: FAM-G<sub>3</sub>AG<sub>3</sub>CGCTG<sub>3</sub>AG<sub>2</sub>AG<sub>3</sub>-Tamra

FKit2T: FAM-G<sub>3</sub>CG<sub>3</sub>CGCGAG<sub>3</sub>AG<sub>4</sub>-Tamra

F25CebT: FAM-AG<sub>3</sub>TG<sub>3</sub>TGTA<sub>2</sub>GTGTG<sub>3</sub>TG<sub>3</sub>T-Tamra

F21RT: FAM-G<sub>3</sub>[U<sub>2</sub>AG<sub>3</sub>]<sub>3</sub>-Tamra

F21CTAT: FAM-G<sub>3</sub>[CTAG<sub>3</sub>]<sub>3</sub>-Tamra

FdxT: FAM-[TA]<sub>2</sub>GC[TA]<sub>2</sub>-hexaethyleneglycol-[TA]<sub>2</sub>GC[TA]<sub>2</sub>-Tamra

**HT-G4-FID experiments:** HT-G4-FID measurements were performed as described previously.<sup>[15b]</sup> TO (thiazole orange) and cacodylic acid were purchased from Aldrich and used without further purification. Stock solutions of TO (2 mM in DMSO) and ligands (500 μM in DMSO) were used for G4-FID assay. Oligonucleotides purified by reverse phase HPLC

were purchased from Eurogentec (Belgium). Sequences: 22AG corresponds to the human telomeric repeat: [5'-AG<sub>3</sub>(T<sub>2</sub>AG<sub>3</sub>)<sub>3</sub>-3']; 21CTA to a modified human telomeric sequence [5'-G<sub>3</sub>(CTAG<sub>3</sub>)<sub>3</sub>-3'];<sup>[25]</sup> *c-kit1* [5'-G<sub>3</sub>AG<sub>3</sub>CGCTG<sub>3</sub>AG<sub>2</sub>AG<sub>3</sub>-3'] and *c-kit2* [5'-G<sub>3</sub>CG<sub>3</sub>(CG)<sub>2</sub>AG<sub>3</sub>AG<sub>4</sub>-3'] are two sequences of the *c-kit* oncogene promoter and *c-myc* [5'-T<sub>2</sub>GAG<sub>3</sub>TG<sub>3</sub>TAG<sub>3</sub>TG<sub>3</sub>TA<sub>2</sub>-3'] of the *c-myc* oncogene promoter; TBA is the thrombin binding aptamer sequence [5'-GGTTGGTGTGGTTGG-3']; ds26 is the duplex obtained with the self-complementary sequence [5'-CA<sub>2</sub>TCG<sub>2</sub>ATCGA<sub>2</sub>T<sub>2</sub>CGATC<sub>2</sub>GAT<sub>2</sub>G-3']. HT-G4-FID measurements were performed on a FLUOstar Omega microplate reader (BMG Labtech) with a 96-wells black quartz microplate (Hellma). The percentage of displacement was calculated from the fluorescence intensity (FA) by using: percentage of displacement = 100 - [(FA/FA<sub>0</sub>) × 100], FA<sub>0</sub> being the fluorescence from TO bound to DNA without added ligand. The percentage of displacement was then plotted as a function of the concentration of added ligand.

**CD spectroscopy:** CD measurements were carried out at 22 °C with a JASCO J-710 spectropolarimeter equipped with a Peltier temperature controller (Jasco PTC-348WI) interfaced to a PC, by using rectangular quartz cells of 1 cm path (1 mL reaction volume). The scans were recorded from 220 to 500 nm with the following parameters: 100 mdeg sensitivity, 1 nm data pitch, 200 nm min<sup>-1</sup> scanning speed, 1 s response, 1 nm band width, 4 accumulations. Solutions containing a constant concentration (5 μM) of G-quadruplex DNA (22-mer human telomeric sequence 22AG) were titrated with increasing amounts of ligands (0 to 6 equiv; 10 min stabilisation time) in either lithium cacodylate (10 mM) supplemented with potassium or sodium chloride (100 mM), pH 7.2, or Tris buffer (50 mM), pH 7.4, in the absence of metallic cation. The scan of the buffer was subtracted from the average scan for each sample. Global fitting (nonlinear regression by the Levenberg–Marquardt algorithm) of scatter plots was performed by using the Hill equation (corrected with fixed offsets) with shared binding and Hill constants. Significance of global fit models was verified by Fisher's and Student's tests.

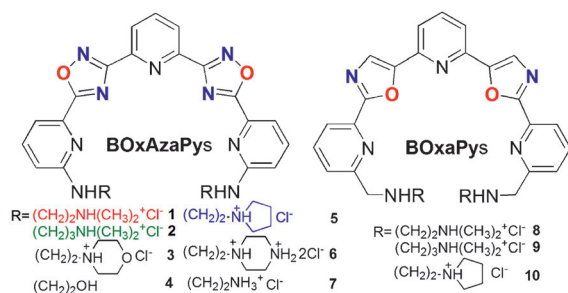
## Acknowledgements

This work was supported by MIUR: PRIN 2009 (2009MFRKZ8), and by the University of Pavia. M.-P.T.-F. gratefully acknowledge Chi-Hung Nguyen for the generous gift of **BoxaPy-CO**, as well as the financial support of the Institut Curie to D.V. and E.L., the CNRS to E.L. and the ANR to F.H. and J.-L.M. (ANR-09-BLAN-0355 "G4Toolbox"). J.-L.M. also acknowledges the Conseil Régional d'Aquitaine, the Fondation pour la Recherche Médicale (FRM) and the foundation ARC for financial support.

- [1] a) S. Balasubramanian, S. Neidle, *Curr. Opin. Chem. Biol.* **2009**, *13*, 345–353; b) D. Monchaud, M. P. Teulade-Fichou, *Org. Biomol. Chem.* **2008**, *6*, 627–636.
- [2] a) L. Delaurière, Z. Y. Dong, K. Laxmi-Reddy, F. Godde, J. J. Toulme, I. Huc, *Angew. Chem.* **2012**, *124*, 488–492; *Angew. Chem. Int. Ed.* **2012**, *51*, 473–477; b) J. Dash, R. N. Das, N. Hegde, G. D. Pantos, P. S. Shirude, S. Balasubramanian, *Chem. Eur. J.* **2012**, *18*, 554–564; c) G. W. Collie, R. Promontorio, S. M. Hampel, M. Micco, S. Neidle, G. N. Parkinson, *J. Am. Chem. Soc.* **2012**, *134*, 2723–2731; d) J. Dash, Z. A. E. Waller, G. D. Pantos, S. Balasubramanian, *Chem. Eur. J.* **2011**, *17*, 4571–4581; e) S. Sparapani, S. M. Haider, F. Doria, M. Gunaratnam, S. Neidle, *J. Am. Chem. Soc.* **2010**, *132*, 12263–12272.
- [3] a) M. Di Antonio, F. Doria, S. N. Richter, C. Bertipaglia, M. Mella, C. Sissi, M. Palumbo, M. Freccero, *J. Am. Chem. Soc.* **2009**, *131*, 13132–13141; b) M. Nadai, F. Doria, M. Di Antonio, G. Sattin, L. Germani, C. Percivalle, M. Palumbo, S. N. Richter, M. Freccero, *Biochimie* **2011**, *93*, 1328–1340; c) F. Doria, M. Nadai, M. Folini, M. Di Antonio, L. Germani, C. Percivalle, C. Sissi, N. Zaffaroni, S. Alcaro, A. Artese, S. N. Richter, M. Freccero, *Org. Biomol. Chem.* **2012**, *10*, 2798–2806.
- [4] a) P. Murat, Y. Singh, E. Defrancq, *Chem. Soc. Rev.* **2011**, *40*, 5293–5307; b) I. M. Dixon, F. Lopez, A. M. Tejera, J. P. Esteve, M. A. Blasco, G. Pratviel, B. Meunier, *J. Am. Chem. Soc.* **2007**, *129*, 1502–1503.
- [5] a) J. Linder, T. P. Garner, H. E. L. Williams, M. S. Searle, C. J. Moody, *J. Am. Chem. Soc.* **2011**, *133*, 1044–1051; b) T. Doi, K. Shibata, M. Yoshida, M. Takagi, M. Tera, K. Nagasawa, K. Shin-Ya, T. Takahashi, *Org. Biomol. Chem.* **2011**, *9*, 387–393.
- [6] a) S. G. Rzuczek, D. S. Pilch, A. Liu, L. Liu, E. J. LaVoie, J. E. Rice, *J. Med. Chem.* **2010**, *53*, 3632–3644; b) C. M. Barbieri, A. R. Srinivasan, S. G. Rzuczek, J. E. Rice, E. J. LaVoie, D. S. Pilch, *Nucleic Acids Res.* **2007**, *35*, 3272–3286; c) K. Jantos, R. Rodriguez, S. Ladame, P. S. Shirude, S. Balasubramanian, *J. Am. Chem. Soc.* **2006**, *128*, 13662–13663; d) M. Tera, K. Iida, K. Ikebukuro, H. Seimiya, K. Shin-ya, K. Nagasawa, *Org. Biomol. Chem.* **2010**, *8*, 2749–2755; e) M. Tera, K. Iida, H. Ishizuka, M. Takagi, M. Suganuma, T. Doi, K. Shin-ya, K. Nagasawa, *ChemBioChem* **2009**, *10*, 431–435; f) K. Iida, M. Tera, T. Hirokawa, K. Shin-ya, K. Nagasawa, *Chem. Commun.* **2009**, 6481–6483.
- [7] F. Hamon, E. Lary, A. Guédin-Beaurepaire, M. Rouchon-Dagois, A. Sidibe, D. Monchaud, J. L. Mergny, J. F. Riou, C. H. Nguyen, M. P. Teulade-Fichou, *Angew. Chem.* **2011**, *123*, 8904–8908; *Angew. Chem. Int. Ed.* **2011**, *50*, 8745–8749.
- [8] a) Y. Wang, R. L. Miller, D. R. Sauer, S. W. Djuric, *Org. Lett.* **2005**, *7*, 925–928; b) V. Santagada, F. Frecentese, E. Perissutti, D. Cirillo, S. Terracciano, G. Caliendo, *Bioorg. Med. Chem. Lett.* **2004**, *14*, 4491–4493.
- [9] a) S. Melato, P. Coghi, N. Basilico, D. Prospero, D. Monti, *Eur. J. Org. Chem.* **2007**, 6118–6123; b) A. G. Takvorian, A. P. Combs, *J. Comb. Chem.* **2004**, *6*, 171–174; c) S. Ding, N. S. Gray, Q. Ding, P. G. Schultz, *J. Org. Chem.* **2001**, *66*, 8273–8276.
- [10] a) J. L. Mergny, J. C. Maurizot, *ChemBioChem* **2001**, *2*, 124–132; b) A. De Cian, L. Guittat, M. Kaiser, B. Sacca, S. Amrane, A. Bourdoncle, P. Alberti, M. P. Teulade-Fichou, L. Lacroix, J. L. Mergny, *Methods* **2007**, *42*, 183–195; c) D. Renčuk, J. Zhou, L. Beaurepaire, A. Guédin, A. Bourdoncle, J. L. Mergny, *Methods* **2012**, *57*, 122–128.
- [11] a) N. H. Campbell, M. Patel, A. B. Tofa, R. Ghosh, G. N. Parkinson, S. Neidle, *Biochemistry* **2009**, *48*, 1675–1680; b) P. Wang, C.-H. Leung, D.-L. Ma, S.-C. Yan, C.-M. Che, *Chem. Eur. J.* **2010**, *16*, 6900–6911.
- [12] a) P. J. Perry, M. A. Read, R. T. Davies, S. M. Gowan, A. P. Reszka, A. A. Wood, L. R. Kelland, S. Neidle, *J. Med. Chem.* **1999**, *42*, 2679–2684; b) C. Martins, M. Gunaratnam, J. Stuart, V. Makwana, O. Greciano, A. P. Reszka, L. R. Kelland, S. Neidle, *Bioorg. Med. Chem. Lett.* **2007**, *17*, 2293–2298; c) W.-J. Zhang, T.-M. Ou, Y.-J. Lu, Y.-Y. Huang, W.-B. Wu, Z.-S. Huang, J.-L. Zhou, K.-Y. Wong, L.-Q. Gu, *Bioorg. Med. Chem.* **2007**, *15*, 5493–5501.
- [13] a) W.-B. Wu, S.-H. Chen, J.-Q. Hou, J.-H. Tan, T.-M. Ou, S.-L. Huang, D. Li, L.-Q. Gu, Z.-S. Huang, *Org. Biomol. Chem.* **2011**, *9*, 2975–2986; b) N. M. Smith, G. Labrunie, B. Corry, P. L. T. Tran, M. Norret, M. Djavaheri-Mergny, C. L. Raston, J.-L. Mergny, *Org. Biomol. Chem.* **2011**, *9*, 6154–6162.
- [14] F. Cuenca, O. Greciano, M. Gunaratnam, S. Haider, D. Munnur, R. Nanjunda, W. D. Wilson, S. Neidle, *Bioorg. Med. Chem. Lett.* **2008**, *18*, 1668–1673.
- [15] a) P. L. T. Tran, E. Lary, F. Hamon, M. P. Teulade-Fichou, J. L. Mergny, *Biochimie* **2011**, *93*, 1288–1296; b) E. Lary, F. Hamon, M. P. Teulade-Fichou, *Anal. Bioanal. Chem.* **2011**, *400*, 3419–3427; c) D. Monchaud, C. Allain, M. P. Teulade-Fichou, *Bioorg. Med. Chem. Lett.* **2006**, *16*, 4842–4845.
- [16] H. Bertrand, D. Monchaud, A. De Cian, R. Guillot, J. L. Mergny, M. P. Teulade-Fichou, *Org. Biomol. Chem.* **2007**, *5*, 2555–2559.
- [17] S. Cosconati, L. Marinelli, R. Trotta, A. Virno, S. De Tito, R. Romagnoli, B. Pagano, V. Limongelli, C. Giancola, P. G. Baraldi, L. Mayol, E. Novellino, A. Randazzo, *J. Am. Chem. Soc.* **2010**, *132*, 6425–6433.

- [18] a) J. S. Hudson, S. C. Brooks, D. E. Graves, *Biochemistry* **2009**, *48*, 4440–4447; b) V. Veglasky, L. Bauer, K. Tluczkova, *Biochemistry* **2010**, *49*, 2110–2120; c) D. Renciuik, I. Kejnovska, P. Skolakova, K. Bednarova, J. Motlova, M. Vorlickova, *Nucleic Acids Res.* **2009**, *37*, 6625–6634; d) G. Gottarelli, S. Lena, S. Masiero, S. Pieraccini, G. P. Spada, *Chirality* **2008**, *20*, 471–485.
- [19] D. M. Gray, J.-D. Wen, C. W. Gray, R. Repges, C. Repges, G. Raabe, J. Fleischhauer, *Chirality* **2008**, *20*, 431–440.
- [20] a) A. T. Phan, K. N. Luu, D. J. Patel, *Nucleic Acids Res.* **2006**, *34*, 5715–5719; b) A. T. Phan, V. Kuryavyi, K. N. Luu, D. J. Patel, *Nucleic Acids Res.* **2007**, *35*, 6517–6525.
- [21] K. Bhadra, G. S. Kumar, *Biochim. Biophys. Acta* **2011**, *1810*, 485–496.
- [22] P. Balagurumoorthy, S. K. Brahmachari, *J. Biol. Chem.* **1994**, *269*, 21858–21869.
- [23] B. A. Bovenzi, G. A. Pearse, *J. Chem. Soc. Dalton* **1997**, 2793–2797.
- [24] a) T. Tsubogo, Y. Kano, K. Ikemoto, Y. Yamashita, S. Kobayashi, *Tetrahedron: Asymmetry* **2010**, *21*, 1221–1225; b) A. M. Tondreau, J. M. Darmon, B. M. Wile, S. K. Floyd, E. Lobkovsky, P. J. Chirik, *Organometallics* **2009**, *28*, 3928–3940.
- [25] K. W. Lim, P. Alberti, A. Guedin, L. Lacroix, J.-F. Riou, N. J. Royle, J.-L. Mergny, A. T. Phan, *Nucleic Acids Res.* **2009**, *37*, 6239–6248.

Received: June 13, 2012  
Published online: ■ ■ ■, 2012



**Oxadiazoles improve binding:** Microwave-assisted synthesis of water soluble acyclic pentaheteroaryls containing 1,2,4-oxadiazoles (**1–7**; see structure) was achieved. The binding with DNA quadruplex structures was investigated

by FRET melting, G4-FID and CD spectroscopy. The oxadiazole containing ligands **1**, **2**, and **5** were better binders than the structurally related oxazoles (**8–10**).

## DNA Recognition

M. Petenzi, D. Verga, E. Largy,  
F. Hamon, F. Doria,  
M.-P. Teulade-Fichou,\* A. Guédin,  
J.-L. Mergny, M. Mella,  
M. Freccero\* .....



## Cationic Pentaheteroaryls as Selective G-Quadruplex Ligands by Solvent-Free Microwave-Assisted Synthesis

